TECHNICAL RESEARCH REPORT

SYSTEMS RESEARCH CENTER

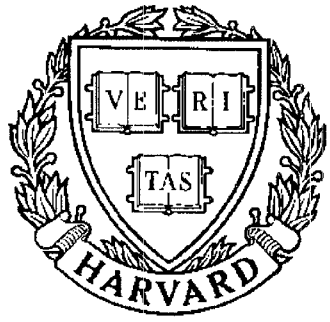

Supported by the National Science Foundation Engineering Research Center Program (NSFD CD 8803012), the University of Maryland, Harvard University, and Industry

A Hidden Markov Model Approach to the Study of Random Tool Motion during Machining

by G.M. Zhang and C. Lin

TR 91-18

A Hidden Markov Model Approach to the Study of Random Tool Motion during Machining

Guangming Zhang and Chien Lin

Department of Mechanical Engineering and Systems Research Center
University of Maryland
College Park, MD 20742

Abstract

This paper presents a new approach to the study of random tool motion during machining. Theory of the hidden Markov model is applied to formulate a comprehensive random excitation system present during machining. Based on the microstructural analysis, characteristics of the hardness distribution in the material being machined are identified for analyzing the cutting dynamics in microscale. The machining action within one revolution of the workpiece and the relation between the machining actions in consecutive revolutions are interpreted as a double stochastic process. Computer simulation based on the hidden Markov model approach is used to predict values of surface roughness characterization indices under given machining conditions. The predictions are compared with the data obtained from direct measurements, showing good agreements. The developed approach has brought new light on a better understanding of vibration control during machining.

1. Introduction

Today's technological innovations in manufacturing are driven by demands to maintain a consistent, high level of product quality in the modern manufacturing environment. Quality of manufactured products such as functionality and reliability depends on finish quality of machined surfaces. Manufacturing engineers are now faced with the difficult problem of improving finish quality without compromising productivity. As a result, research on the control of finish quality of machined surfaces has attracted great attention.

It has been well known that the roughness profile of a machined surface contains periodic and nonperiodic components. The geometry of machining action is responsible for the generation of the periodic components. During a turning operation, the spindle speed, machining feed and tool geometry determine a spiral tool path. However, random tool motion during machining aggravates the surface texture formation. Factors, which cause the tool vibration in a random manner, could be built-up edges, tool wear, and nonhomogeneity of basic material properties. Evaluation and control of tool vibration, for both deterministic and stochastic parts, have been the focus for improving finish quality of machined surfaces.

Results from previous research have strongly suggested the use of precise spindle and feed mechanisms for machining error reduction [1-2]. Work on machine tool accuracy enhancement has been successfully improving the rigidity of machine tool structures or/and compensating the deterministic part of tool path errors during machining [3-5]. Study on measurement and assessment of topography of machined surfaces has been extensive [6-7]. Methods like wavelength decomposition of surface roughness [8], time series modeling of machined surfaces [9], and surface models from light scattering measurements [10] were developed for establishing the relationship between surface parameters and pertinent machining parameters. A recent study indicated that the nonhomogeneity of basic material properties, such as hardness, could be one of the major sources to excite random tool motion during machining [11-12]. Research has been conducted to establish a mapping function between the variability of standard material properties and the formation of surface irregularities.

The work presented in this paper represents a continuation of the research effort for evaluating random tool motion during machining. A statistic method of hidden Markov modeling is applied to describe the random excitation phenomenon. The developed model employs two stochastic processes to formulate the mechanism of random excitation. The first stochastic process characterizes the random tool motion within a single revolution of the workpiece. The second stochastic process quantifies the interrelationship of random tool motion between the consecutive revolutions of the workpiece. Analysis of the cutting dynamics in microscale under the formulated random excitation provides rich information about possible strategies for controlling the quality of machined surfaces.

The paper is organized as follows. Section 2 presents the modeling process of random excitation. The nonhomogeneity of hardness distribution in the workpiece material is assumed to be a major random excitation source. Concepts of the segment excitation and overall excitation are defined to form a basis for the development of a hidden Markov model to describe the random excitation observed during machining. Section 3 presents a technical detail about determination of the states and state transition matrix. Computer implementation is also discussed in this section. A case study is presented in section 4 to demonstrate the procedure to apply the developed hidden Markov model for the study of random tool motion during machining. Discussion of results is given in section 5 where results from the experimental work are compared with the predictions based on the hidden Markov modeling approach. Effects of the state selection and state transition matrix on

random tool motion are investigated through a two-level factorial design. Section 5 contains concluding remarks.

2. Basic Methodology

Random tool motion, a phenomenon observed in the production line, has been blamed as a major element to deteriorate product quality. Research on a quantitative identification of the random excitation source still remains as a challenge to the manufacturing community. In this research, we assume that the nonhomogeniety of basic material properties, such as material hardness, is of primary importance to cause random tool motion during machining.

2.1 Random Tool Motion

Figure 1 presents an intuitive view to explain the mechanism that a nonhomogeneous distribution of the material being machined could excite random tool motion during machining. The individual blocks in Fig. 1 represent volumes of the material being removed at time intervals Δt. From the machining point of view, the cutting force generated at these time intervals is related to the hardness of the volume material. It is evident that the cutting force varies as the hardness value of an individual block varies. The variation of the cutting force, which is of random nature, introduces random tool vibration during machining. It becomes necessary to characterize the hardness distribution of material for the evaluation of random tool motion.

2.2 Microstructural Analysis

It has been known that the hardness distribution of material in microscale is characterized by the size, shape, and segregation of the microstructures present in material. Figures 2a and 2b are photographs of the microstructures in an SAE 72 carbon steel bar. Figure. 2a illustrates the microstructural distribution observed in a cross-section perpendicular to the bar axis, and Fig. 2b the microstructual distribution observed in the cross-section along the bar axis. The dark and white parts stand for pearlite and ferrite structures, respectively. Comparing the microstructures displayed in Fig. 2a and Fig. 2b, the sizes of pearlite structure shown in Fig. 2a are relatively small and their shapes look irregular. On the other hand, the pearlite structures in Fig. 2b are shown as narrow strips. These narrow strips are distributed in parallel, depicting a distribution pattern. This narrow and parallel strip pattern results from the rolling process when the SAE 72 carbon steel was fabricated. Due to the fact that the hardness of pearlite structure is much higher than the

hardness of ferrite structure, patterns of a nonhomogeneous distribution of microstructures lead to patterns of a nonhomogeneous distributions of hardness correspondingly. During the machining of carbon steel materials, the presence of a nonhomogeneous distribution of hardness gives rise to variation of the cutting force, which causes the tool to randomly vibrate.

2.3 Hidden Markov Modeling

Theoretically speaking, a hidden Markov model is a doubly stochastic process with an underlying stochastic process that is not observable (it is hidden), but can only be observed through another set of stochastic processes that produce the sequence of observed events.

The strategy of modeling random excitation is to view the random excitation during the machining of carbon steel materials as a direct concatenation of "short time" random excitation segments. Each of "short time" random excitation segments represents the random excitation action during one revolution of the workpiece. The statistical model for the segment excitation is subjected to the hardness distribution observed in the cross-section of the material being machined, i.e., the one shown in Fig. 2a. The overall excitation action is a synchronous sequence of these segments. Therefore, it can be described by a hidden Markov model. The statistical model to represent the transition process from one segment to the consecutive segment is subjected to the hardness distribution in the machining feed direction, i.e., the one shown in Fig. 2b. As a result, the random excitation during the entire machining process is considered to be a doubly embeded stochastic process.

2.3.1 Modeling of Segment Excitation

Imagining that the machining process is to take individual blocks away from the workpiece material, the ratio of pearlite structure to ferrite structure within the block being removed varies from one block to another. Meanwhile, the cutting force follows the ratio variation to vary, forming a microscale random excitation.

A statistical model to describe this excitation action was developed and reported in [11]. Development of the reported statistical model was based on an assumption, i.e., the excitation action at a specific machining instant was determined by the mean hardness value of the block being removed. Due to the nonhomogeneous hardness distribution, the parameter of block mean hardness was treated as a random variable, which was assumed to obey a normal distribution because of the central limit theorem in statistics. The mean and

variance of the normal distribution for modeling the variation of mean hardness values were calculated through microstructural analysis, as briefly discussed in section 2.2.

In this research, this reported statistical model is used to characterize the segment excitation action, or the excitation action within one revolution of workpiece. For given mean and variance values of the statistical model and the number of blocks divided along the workpiece circumference, one can construct a data set, using a random number generator on a computer, to represent the block mean hardness variation along the workpiece circumference, or within one revolution of the workpiece.

2.3.2 Modeling of Overall Excitation

As discussed above, the segment excitation model characterizes the effect of the nonhomogeneous distribution of hardness on the variation of the cutting force during one revolution of the workpiece. If examining the distribution pattern shown in Fig. 2b, which is viewed along the machining feed direction, the concurrence of different microstructures appearing in the neighboring areas, or in the consecutive revolutions of the workpiece, can be observed. This concurrence is directly related to the narrow strips of pearlite and characterized by

1. the presence of a hard (or soft) spot on a specific circumferential location is correlated with the presence of a hard (or soft) spot on its consecutive, or neighboring locations, and
2. in a general case, the changing process, which is from a hard (or soft) spot to the soft (or the hard) spot is gradually proceeding, although the abrupt jumps between an extreme hard and an extreme soft spots, or vice versa, occasionally happen.

To further clarify the two observations, Fig. 3 illustrates a state-transition representation. The entire area of the microstructural photograph shown in Fig. 2b was divided into 12 equal gridblocks. Each gridblock represented an area of 0.14 x 0.14 mm^2. Using electronic scanning, the numbers of pearlite and ferrite within each of the 12 gridblocks were identified and listed in the corresponding gridblock. The mean hardness values of the 12 gridblocks were calculated where the hardness values of pearlite and ferrite structures were assumed to be 150 BHN and 38 BHN, respectively. It is evident that the mean hardness value varies from one gridblock to another. If we assume that gridblock A-1 ($\mu_{A\text{-}1}$ = 122 BHN) represents a soft spot location and gridblock B-1 ($\mu_{B\text{-}1}$ = 132 BHN) a hard spot location, an observation can be made that the variation of the mean hardness

values on row A ranges from 122 BHN to 121 BHN and the variation of the mean hardness values on row B ranges from 132 BHN to 121 BHN. This observation again confirms that along the machining feed direction, the appearance of a hard (or soft) spot location on the circumferential direction is constrained by its neighboring hardness status. In order to evaluate the overall excitation action during machining, there is a pressing need to formulate a statistical method to describe the distribution pattern of the mean hardness values in the consecutive locations along the machining feed direction. In this research, theory of hidden Markov modeling is used to extend the segment excitation model into a comprehensive random excitation model.

3. Determination of States and State Transition Matrix

In the theory of hidden Markov modeling, the possible outcomes of a stochastic process are classified as events. The basic principles of hidden Markov modeling are using an observable stochastic process to toss the outcome (one of the classified events) and using an underlying stochastic process to add a specific constraint on the likelihood of the concurrence of different states. This constraint is called "state transition matrix".

3.1 Determination of States of Segment Excitation

In this research, the segment excitation model is considered to be the observable stochastic process. If the number of blocks on the circumferential direction is assumed to be N_s, the N_s mean hardness values, i.e., μ_1,μ_2,μ_3, ..., μ_{Ns-1},μ_{Ns}, obey a normal distribution shown in Fig. 4. Now we classify the N_s mean hardness values into *n* states and each of the *n* states covers a certain range of the mean hardness values. As indicated in Fig. 4, the probability associated with each of the *n* states is given by ratio of the number of those mean hardness values falling into its corresponding interval to the block number N_s, and the probabilities associated with the *n* states for the N_s blocks, or within one revolution of the workpiece, are governed by

$$\sum_{i=1}^{n} P_i = 1$$

As an example to demonstrate the formation of a four (4) state segment excitation , we assume that the material being removed from the workpiece circumference during one revolution is divided into 50 blocks. The mean (μ) and standard deviation (σ) of the normal distribution associated with the 50 block mean hardness values are 125 BHN and 12 BHN, respectively. Figure 4 actually depicts this normal distribution. Within the range

$[\mu - 3\sigma, \mu + 3\sigma]$ or [89, 161], four cells with an equal span $\frac{3\sigma}{2}$ are formed. As illustrated, state 1 covers the mean hardness values from 89 BHN to 107 BHN. There are 4 mean hardness values falling into this cell. The probability associated with state 1, P_1, is 0.08. In a similar manner, we determine $P_2 = 0.42$, $P_3 = 0.42$, and $P_4 = 0.08$.

3.2 Determination of State Transition Matrix

Serving as the second, or the hidden, stochastic process, the state transition matrix describes both the neighboring and global state transitions. In formulating this matrix, the following two assumptions are made in this research.

1. The next state entered in the hidden stochastic process depends only on the current state, not on the previous states.
2. The transition that can occur is within two adjacent states, implying that the transition is bi-directional. However, the two states on the extremely right and left boundaries are exceptional. Their transitions are unidirectional.

Figure 5a is the state diagram illustrating the model for the neighboring state transition where state 1 represents the state on the left boundary and state 2 is a bi-directional transition state. As illustrated in Fig. 5a, parameter a_1 denotes the transition probability from state 1 to state 1 (itself), parameter a_2 denotes the transition probability from state 2 to state 2 (itself), parameter $(1\text{-}a_1)$ denotes the transition probability from state 1 to state 2, and parameter b_1 denotes the transition probability from state 2 to state 1. As a demonstration example, let us assume that $a_1 = 0.7$, $(1 - a_1) = 0.3$, $a_2 = 0.4$, $b_1 = 0.3$, and $(1 - a_2 - b_1) = 0.3$. Physical interpretations of these given transition probabilities during the transition process are as follows.

1. There are only two possibilities for state 1 to transit, either to remain its original state, or to become state 2. The likelihood for state 1 to stay in its original state is 0.7 and the likelihood for state 1 to transit to state 2 is 0.3.
2. There are three possibilities for state 2 to transit, either to remain its original state, or to become state 1, or to become state 3. The likelihood for state 2 to stay in its original state is 0.4, the likelihood for state 2 to transit to state 1 is 0.3, and the likelihood for state 2 to transit to state 3 is 0.3.

After having developed the model for the neighboring state transition, an *n*-state model for the global state transition can be established. Figure 5b is the state diagram

illustrating the global n-state transition. In Fig. 5b, parameter a_i denotes the transition probability from state i to state i (itself), parameter b_i denotes the transition probability from state i to state (i-1), and parameter $(1 - a_i - b_{i-1})$ denotes the transition probability from state i to state (i+1). The neighboring and global state transition diagrams shown in Fig. 5a and 5b can be explicitly represented in a matrix form. Such a matrix is called state transition matrix. Its basic structure is provided below.

$$
\begin{array}{c}
 \\ \mathbf{1} \\ \mathbf{2} \\ \cdot \\ \cdot \\ \\ \mathbf{n-1} \\ \mathbf{n}
\end{array}
\begin{array}{c}
\begin{array}{cccccc}
\mathbf{1} & \mathbf{2} & \cdots & & \mathbf{n-1} & \mathbf{n}
\end{array} \\
\left[\begin{array}{cccccc}
a_1 & 1 - a_1 & \cdots & & 0 & 0 \\
b_1 & a_2 & 1 - a_2 - b_1 & \cdots & & 0 \\
0 & b_2 & a_3 & \cdots & & \\
0 & & & & & \\
 & & & & & 0 \\
0 & & \cdots & b_{n-2} & a_{n-1} & 1 - a_{n-1} - b_{n-2} \\
0 & 0 & \cdots & 0 & 1 - a_n & a_n
\end{array}\right]
\end{array}
$$

In the state transition matrix, the elements on the diagonal represent the transition probabilities of remaining their original states, and the off-diagonal elements represent the probabilities of transiting from one state to another. The bandwidth of the transition matrix, which is equal to three (3) in the above matrix, reflects the assumption made for the neighboring state transition. Therefore, the transition matrix characterizes the unobservable, or the hidden, stochastic process.

3.3 Determination of Transition Probabilities

As discussed in section 2.4.1, to determine P_i for i = 1, 2, ..., n, we may group the mean hardness values of $\mu_1, \mu_2, \mu_3, \ldots, \mu_{Ns-1}, \mu_{Ns}$ into their corresponding state cells. An experimental procedure is developed to determine the state transition probabilities, i.e., a_i, b_i, and $(1 - a_i - b_{i-1})$ for i = 1, 2, ..., n. The procedure consists of three steps.

Step 1. Select a representative sample along the machining feed direction from the material to be machined. Use a computer-based scanning and imaging process to identify the type of microstructure at each location in the representative

sample. Measure the microhardness value for each of the identified microstructures.

Step 2. Construct the gridblocks. The gridblock dimension should be determined by the number of blocks assumed on the workpiece circumference and the machining feed to be used during machining. Count the numbers of pearlite and ferrite structures within each of the formed gridblocks. Calculate the mean hardness value for each gridblock. Examine the variation among the calculated mean hardness values to confirm the number of states which was selected in the modeling of segment excitation. Otherwise, a proper adjustment for the number of states should be taken. At this stage, a state transition description, which is similar to the one shown in Fig. 3, is completed.

Step 3. Determine the transition probabilities, i.e.,a_i, b_i, and $(1 - a_i - b_{i-1})$ for i = 1, 2, ..., n.. In this initial research, we assume that transition probabilities, a_i, b_i, and $(1 - a_i - b_{i-1})$ for i = 2,3, ..., n-1, are equal to each other. The transition probabilities associated with the two extreme boundary states are defined as $a_1 = (a_2 + b_1)$ and $a_n = (a_{n-1} + b_{n-1})$ because these two states are unidiretional states. Referring to the state transition representation shown in Fig. 3, we may select $a_i = 0.4$ for i = 2,3,...,n-2,n-1, $b_i = 0.3$ for i = 1,2,...,n-1, $a_1 = 0.7$, and $a_n = 0.7$.

3.4 Implementation on Computer

The basic methodology for modeling a comprehensive random excitation is based on the hidden Markov modeling theory. A computer program was developed to implement this methodology on a computer. The block diagram shown in Fig. 6 outlines the simulation strategy, which is built upon four modules, i.e., the user input module, the segment excitation module, the state transition module, and the output module. Note that the data from the output module represents the random excitation action, which will be used as an input function to the program called "evaluation of random tool motion", which was developed in [14]. The descriptions of these four modules are given below.

1. The user input module. To initiate the computer simulation, the following parameter values should be specified through the designed user interface.
   (1). The mean and standard deviation of the segment excitation model, i.e., μ and σ.
   (2). The block number selected for the segment excitation model, N_s, and the number of states selected for the state transition matrix, *n*.

(3). The transformation probabilities, i.e., a_i for i = 1,2,3,...,n-1,n, and b_i for i = 1,2,...,n-1.

(4). The number of workpiece revolutions to be simulated.

(5). The control parameters such as the variation levels of μ and σ for each revolution of the workpiece.

2. The segment excitation module. A random number generator is built to construct the normal distribution, $N(\mu,\sigma^2)$, which is associated with the block mean hardness values. These generated values are then distributed to individual blocks resembling the workpiece material being removed at specific instants. A built-in divider forms the *n* state groups and assigns the state number to each block. This completes the random excitation simulation for the first workpiece revolution.

3. The state transition module. For the second workpiece revolution and those revolutions to follow, the block mean hardness values are generated using the state transition matrix, instead of using the random number generator built in the segment excitation module. Using the state assignments for the first workpiece revolution as the initial condition, an algorithm is developed to assign the state number to the neighboring location in accordance with the given state transition probabilities. In order to maintain the mean and standard deviation of the assigned block mean hardness values, which also obey a normal distribution, a control scheme is used to regulate the selection of a block mean hardness value from its group. When the assignment for the second revolution is completed, these assigned values will serve as the initial condition to assign new block mean hardness values for the third workpiece revolution. The reiteration of this process completes the second, or the hidden, stochastic process.

4. The output module. It calculates the mean and standard deviation of the assigned block mean hardness values for each revolution of the workpiece, check the normality of the data distribution, and prints out the simulation results. The table attached to Fig. 6 was taken from the state transition representation obtained through computer simulation. This state transition representation and its corresponding block mean hardness values will be used as an input to the computer program designed for simulating tool vibration during machining and the surface topography after machining.

4. A Case Study

A turning operation to machine an SAE 72 steel bar (diameter = 80 mm and length = 300 mm) was studied to demonstrate an application of the hidden Markov model

approach for controlling tool vibration during machining. The study consists of experimental work and computer simulation.

4.1 Experimental Work

First, microstructural analysis, as shown in Fig. 2a and 2b, was performed to quantify the microstructural distribution in the SAE steel bas. Based on the experimental data, the mean and standard deviation used in the segment excitation model and the probabilities of the state transition matrix were estimated. Second, turning test shown in Fig. 1 were carried out on a Placemaker lathe. The machining parameter settings used were feed = 0.23 mm/rev, depth of cut = 0.5 mm, and spindle speed = 470 rpm. After machining, twenty-five (25) surface profiles were taken along the axial direction on a Talysurf 6 surface profilometer. The measured surface profiles were positioned in parallel to form a surface topography. Figure 7a presents the experimental results. The twenty-five measured R_a values, together with $\overline{R_a}$ = 4.22 μm and σ_{Ra} = 0.32 μm, were listed in Table 1.

4.2 Study of Random Tool Motion

Following the experimental work, the developed computer program was used to study random tool motion and its effect on the surface texture formation during machining. The block diagram shown in Fig. 6 illustrates how the basic methodology discussed in section 2 is implemented for the evaluation of random tool motion. As illustrated in Fig. 6, the program named as "evaluation of random tool motion" takes the nominal chip load, the residual chip load due to overlapping machining, and the random excitation as the system inputs to evaluate the tool vibratory response. It combines the evaluated tool motion with the spiral trajectory tool path to generate the data base for constructing the topography of a machined surface [12].

In the computer simulation , the machining parameters used were set identical to those used in the experimental work. In the first simulation run, the input of random excitation only takes the segment excitation into consideration. This means that the random number generator in the segment excitation module was used to generate the block mean hardness values for the first workpiece revolutions, which obeyed the specified normal distribution. Also, the segment excitation module was used to generate the block mean hardness values for the consecutive workpiece revolutions, and the state transition module was skipped during the first simulation run. As a result, there were no constraints which were imposed between the neighboring block mean hardness values along the machining

feed direction. In fact, the first simulation run duplicated the research work reported in [11-12] where random excitation was considered, but only accounted for the nonhomogeneity of the hardness distribution in the cross-section perpendicular to the bar axis. Effect of the nonhomogeneity of the hardness distribution along the machining feed direction was neglected in the previous work [11-12]. Figure 7b presents the simulation results, showing the surface topography through computer visualization. The corresponding R_a values calculated from the simulated surface profiles, together with $\overline{R_a}$ = 3.92 μm and σ_{Ra} = 0.13 μm, were listed in Table 1.

In the second simulation run, the input of random excitation takes both the segment excitation and overall excitation into consideration. During the simulation process, the segment excitation module was used to generate the block mean hardness values only for the first revolution. Afterwards, the state transition matrix was used to generate the block mean hardness values for the rest of workpiece revolutions. The defined transition probabilities, serving as an imposed constraint, supervise the assignments of the block mean hardness values. The assignment process simulates a direct concatenation of the local segment excitation actions, resembling a hidden Markov chain action. This entire simulation process represents a comprehensive study of the effect of the nonhomogeneity of the hardness distribution of the material being machined on the surface texture formation during machining. Figure 7c presents the simulation results. The corresponding R_a values calculated from the simulated surface profiles, together with $\overline{R_a}$ = 4.24 μm and σ_{Ra} = 0.17 μm, were listed in Table 1.

4. Discussion of Results

4.1 Comparison between the Measured and Simulated Topographies.

The two surface topographies shown in Figs. 7b and 7c provide a qualitative visualization of the effect of random tool motion on the surface irregularity generation. In this research, nonhomogeneous distributions of the basic material properties, such as hardness, were assumed to be the major excitation source. A main difference between the two surface topographies can be observed if examining them carefully. The difference is that the surface topography shown in Fig. 7c displays a gentle variation of the profile heights. Such a gentle trend comes from the cohesive relationship of random excitation actions between the consecutive revolutions during machining. This cohesive relation indicates that the likelihood for the occurrence of strong (or a weak) excitation actions at

neighboring locations is higher than the likelihood of the mixed occurrence of strong and weak excitation actions at neighboring locations. Therefore, the simulated Markov chain characterizes the effect of the narrow and parallel pearlite strip pattern of the microstructural distribution on random tool motion during machining. In fact, the gentleness of profile height variation can also be seen from the measured surface topography shown in Fig. 7a. The two surface profiles shown in Fig. 8a and Fig. 8c, which were taken from the two corresponding surface topographies, clearly depict a slow variation pattern of the profile heights. The similarity between the measured topography (Fig. 7a) and the simulated surface topography (Fig. 7c) confirms the validity of proposing the hidden Markov modeling approach for the study of random tool motion during machining.

On the other hand, a high level of variation among the profile heights shown in Fig. 7b can be observed. This is due to the fact that random excitation action was evaluated on a single revolution basis. The random excitation actions between two consecutive workpiece revolutions are considered to be independent of each other. Consequently, the occurrence of a strong (or weak) excitation action at a given location does not impose a condition that a rather strong (or weak) excitation action will occur in its neighboring locations. In fact, the likelihood of having a strong, or a weak, excitation action, in its neighboring location, is solely governed by the segment excitation model which is characterized by a normal distribution. The surface profile shown in Fig. 8b, which was taken from its surface topography, depicts a rather significant variation of the profile heights if compared with those shown in Figs. 8a and 8c. Although more discrepancies can be observed if comparing with the measured surface topography shown in Fig. 8a, the surface topography shown in Fig. 8b would still be a good representation for machining certain carbon steel materials having relatively small and spherical pearlite structures as opposed to the narrow strips of pearlite in the present case study.

4.2 Effects of State Selection and Transition Probabilities

As discussed above, the block mean hardness values within one workpiece revolution are grouped into the state cells for implementation of the state transition matrix. The number of states and the associated transition probabilities were determined mainly based on the results from microstructural analysis. In order to extend our understanding of using the hidden Markov modeling method to formulate the random excitation observed during machining, a two-level factorial design was utilized to investigate the effects of the state selection and transition probability setting on the evaluation of random tool motion during machining. The LOW and HIGH levels of the state selection were set at 4 and 10,

respectively. The low and high levels of the transition probability setting used were (a_i = 0.4 for i = 2,3,...,n-2,n-1, b_i = 0.3 for i = 1,2,...,n-1, a_1 = 0.7, and a_n = 0.7), and (a_i = 0.6 for i = 2,3,...,n-2,n-1, b_i = 0.2 for i = 1,2,...,n-1, a_1 = 0.8, and a_n = 0.8) where the number of the select states is equal to either 4 or 10. Four computer simulation runs were performed using the two-level factorial design. The simulation results in terms of the predicted $\overline{R_a}$ and σ_{Ra} values were given below.

Predictions μm	Run 1 (LOW, low)	Run 2 (LOW, high)	Run 3 (HIGH, low)	Run 4 (HIGH, high)
$\overline{R}_a$	4.24	3.87	3.70	3.67
σ_{Ra}	0.17	0.18	0.02	0.02

Examining the simulation results, the combination of a LOW level of the state selection and a low level of the transition probability setting resulted in the highest value of the $\overline{R_a}$ prediction, which is listed as 4.24 μm. Accordingly, the combination of the HIGH and high levels yielded the smallest value of the $\overline{R_a}$ prediction (3.67 μm). Regarding the σ_{Ra} estimations, it is interesting to note that the low and high levels of the transition probability settings have an unobservable effect on the σ_{Ra} estimation. From the viewpoint of hidden Markov modeling, this phenomenon could be due to the fact that the transition probability setting is related to the hidden stochastic process, which generates patterns along the machining feed directions. At a given state selection, the random hardness valuess generated by the two transition probability settings maintain the R_a variation at a similar level. This phenomenon deserves a further study. Another interesting observation is that the change of the state selection from a LOW level to a HIGH level has a more significant effect on the $\overline{R_a}$ and σ_{Ra} predictions than the change of the transition probability setting does. This indicates that great attention should be paid to a proper selection of the number of the states because the number of states determines the possible patterns which can be observed during the state transition process.

5. Conclusions

1. As a new and innovative approach, the theory of hidden Markov modeling is applied to study the phenomenon of random tool motion caused by the nonhomogeneity of hardness distribution in the material being machined. The general random excitation during machining is viewed as a series of segment excitation during individual revolutions of the workpiece, and the relationship between the segment excitation actions is governed by the state transition process.
2. The segment excitation and the state transition process are modeled as two stochastic processes. The stochastic process to describe the segment excitation, serving as the observable stochastic process, is characterized by a normal distribution with its mean standing for the material hardness in general and its standard derivation representing nonhomogeneity of the hardness distribution. The distribution pattern of microstructures is used to establish the state transition matrix, which characterizes the cohesive relationship between random excitation actions in the consecutive workpiece revolutions. The state transition matrix maneuvers the likelihood of concurrence of different states of the random excitation action, resembling a so-called hidden stochastic process.
3. A prototype system to implement the hidden Markov model on a computer is developed for the study of random tool motion and its effect on the surface texture formation during machining. To confirm the validity of the proposed approach, predictions through computer simulation are compared with the results from the experimental work. A general match between them has been observed.

Acknowledgements

The authors acknowledge the support of the Systems Research Center under Engineering Research Centers Program: NSFD CDF 8803012, and the support of Minta Martin funding from the College of Engineering. They wish to thank Professor W. L. Fourney, Chairman of the Mechanical Engineering Department, and Professor D. K. Anand, Director of the Advanced Design and Manufacturing Laboratory for their valuable support in conducting this work. The technical assistance from the Precision Engineering Division of the National Institute of Standards and Technology and Mr. T. W. Hwang at the University of Maryland is appreciated.

References

1. Kohno, T., Okazaki, Y., Pzawa, N., Mitui, K., and Omoda, M., 1989, "In-Process Measurement and a Workpiece-Referred Form Accuracy Control System (WORFAC): Concept of the Method and Preliminary Experiment," Precision Engineering, Volume 11, Number 1, January 1989, pp. 9-14.
2. Blaedel, K.L., "Error Reduction," in Technology of Machine Tools: Machine Tool Accuracy", Vol. 5, Lawrence Livermore National Laboratory, Livermore, CA, 1980.
3. Tobias, S., "Machine Tool Vibration Research," International Journal of Machine Tool Design and Research, Vol. 1, 1961, pp. 1-14.
4. Tlusty, J. and Ismail, F., "Special Aspects of Chatter in Milling," Journal of Vibration, Acoustics, Stress, and Reliability in Design, ASME Trans., Vol. 105, 1983, pp. 24-30.
5. Donmez, M.A., Bolmquist, D.S., Hocken, R.J., Liu, C.R., and Barash, M.M., "A General Methodology for Machine Tool Accuracy Enhancement by Error Compensation", Precision Engineering, No. 4, 1986.
6. Nayak, P.R., "Some Aspects of Surface Roughness Measurement," Wear, Vol. 26, 1973, pp. 165-174.
7. Zhou, G.Y., Leu, M.C., and Dong, S.X., "Measurement and Assessment of Topography of Machined Surfaces," ASME PED.-Vol. 46, pp. 89-100, 1990
8. Pandit, S.M., and Revach, S., "A Data Dependent System Approach to Dynamics of Surface Generation in Turning," Journal of Engineering for Industry, ASME Trans., Vol. 103b, 1981, pp. 437-445.
9. Kapoor, S.G., and Wu, S.M., "A Stochastic Approach to Paper Surface Characterization and Printability Criteria," Journal of Physics, Vol. 11, 1978, pp. 83-96.
10. Vorburger, T.V., and Scace, B., "Progress Report of the Quality in Automation Project for FY89," NISTIR 4322, National Institute of Standards and Technology, May 1990.
11. G. M. Zhang and S. G. Kapoor, "Dynamic Generation of the Machined Surface, Part I: Mathematical Description of the Random Excitation System," to appear in the Journal of Engineering for Industry, Transactions of ASME, May 1991.
12. Zhang, G. M., and Kapoor, S. G., "Dynamic Generation of the Machined Surface, Part II: Mathematical Description of the Tool Vibratory Motion and Construction of Surface Topography," to appear in the Journal of Engineering for Industry, Transactions of the ASME, May 1991.

13. L. R. Rabiner and B. H. Juang,"An Introduction to Hidden Markov Models," IEEE ASSP Magazine, January 1986, Vol. 3, pp 4-16.
14. G. M. Zhang and T. W. Hwang, "Analysis of the Cutting Dynamics in Microscale," Symposium on Fundamental Issues in Machining, 1990 ASME Winter Annual Meeting, PED-Vol. 43, pp. 25-37.

List of Table

List of Figures

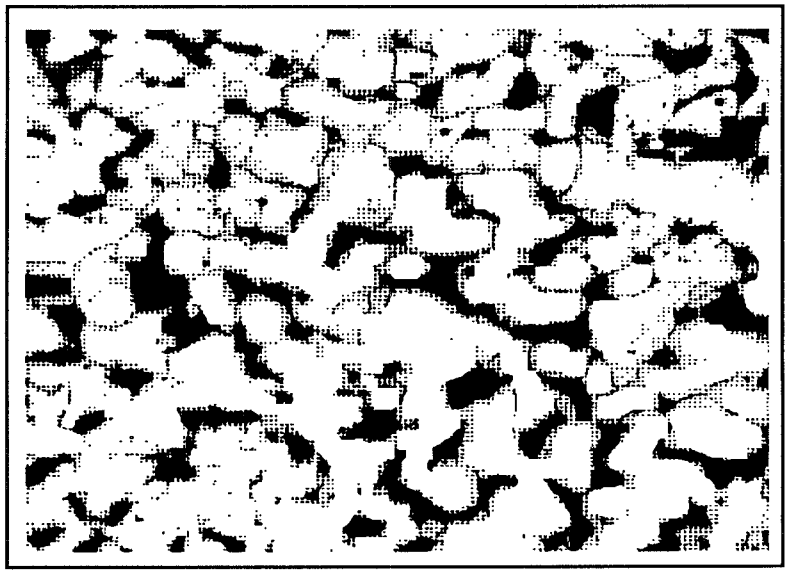

a. Microstructural Distribution in the Cross-Section

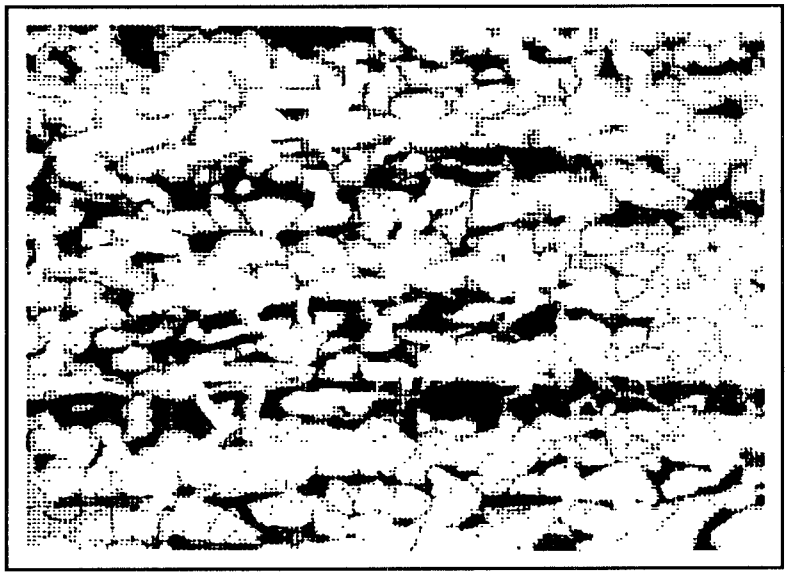

b. Microstructural Distribution along the Axial Direction

Figure 2 Microstructural Analysis

	1	2	3	4
A	No. of Pearlite =88093 No. of Ferrite = 28347 Mean Hardness Value = 122.7	No. of Pearlite =87533 No. of Ferrite = 28907 Mean Hardness Value = 122.2	No. of Pearlite =86824 No. of Ferrite = 29616 Mean Hardness Value = 121.5	No. of Pearlite =86907 No. of Ferrite = 29533 Mean Hardness Value = 121.6
B	No. of Pearlite =98549 No. of Ferrite = 17891 Mean Hardness Value = 132.8	No. of Pearlite =93815 No. of Ferrite = 22625 Mean Hardness Value = 128.3	No. of Pearlite =93382 No. of Ferrite = 23058 Mean Hardness Value = 127.8	No. of Pearlite =86685 No. of Ferrite = 29755 Mean Hardness Value = 121.4
C	No. of Pearlite =97866 No. of Ferrite = 18574 Mean Hardness Value = 132.1	No. of Pearlite =91869 No. of Ferrite = 24571 Mean Hardness Value = 126.4	No. of Pearlite =95741 No. of Ferrite = 20699 Mean Hardness Value = 130.1	No. of Pearlite =85026 No. of Ferrite = 31414 Mean Hardness Value = 119.8

Fig. 3. The Block Mean Hardness Values Calculated from Photograph Fig. 2b

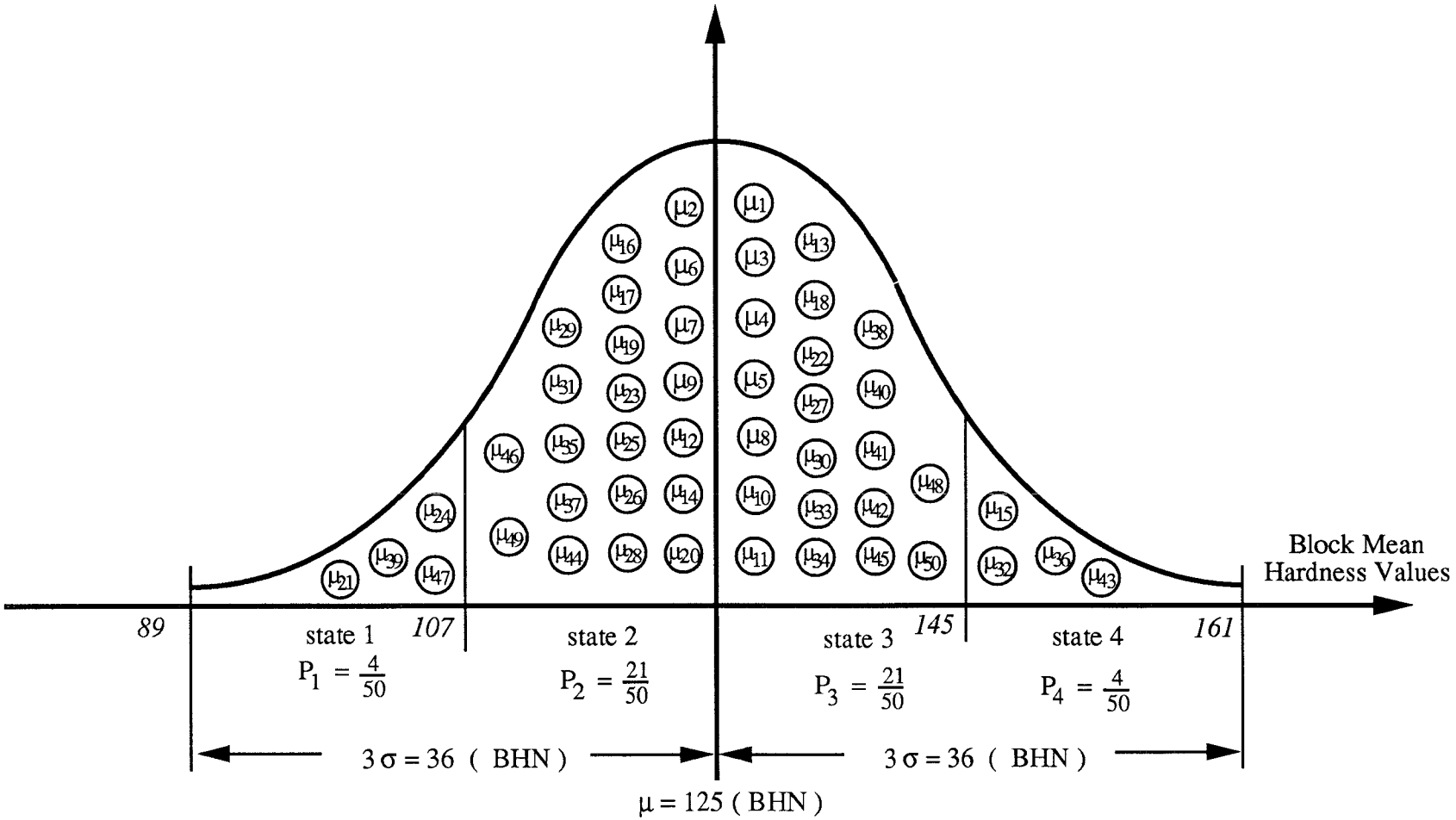

Fig. 4. Normal Distribution N (125, 12^2) for Segment Excitation (Block Number = 50)

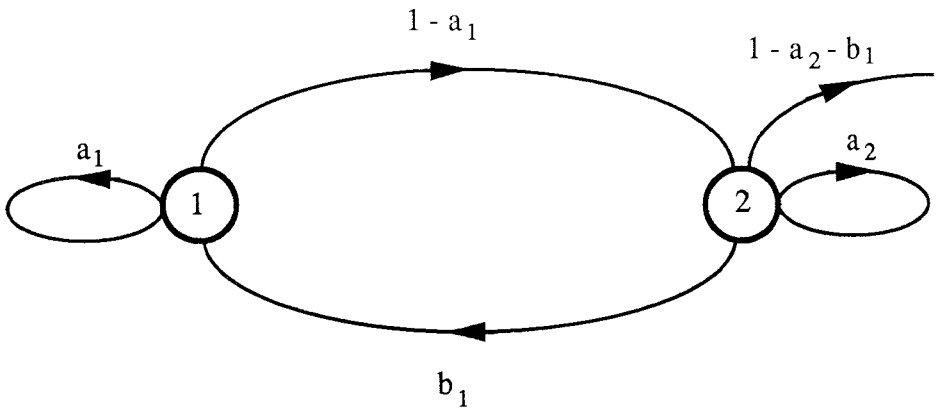

(a) Neighboring state transition diagram

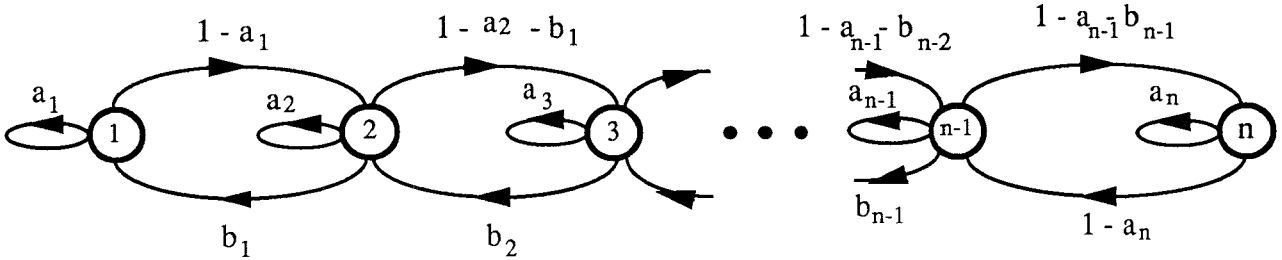

(b) Global n-state transition diagram

Fig. 5. State Transition Diagrams

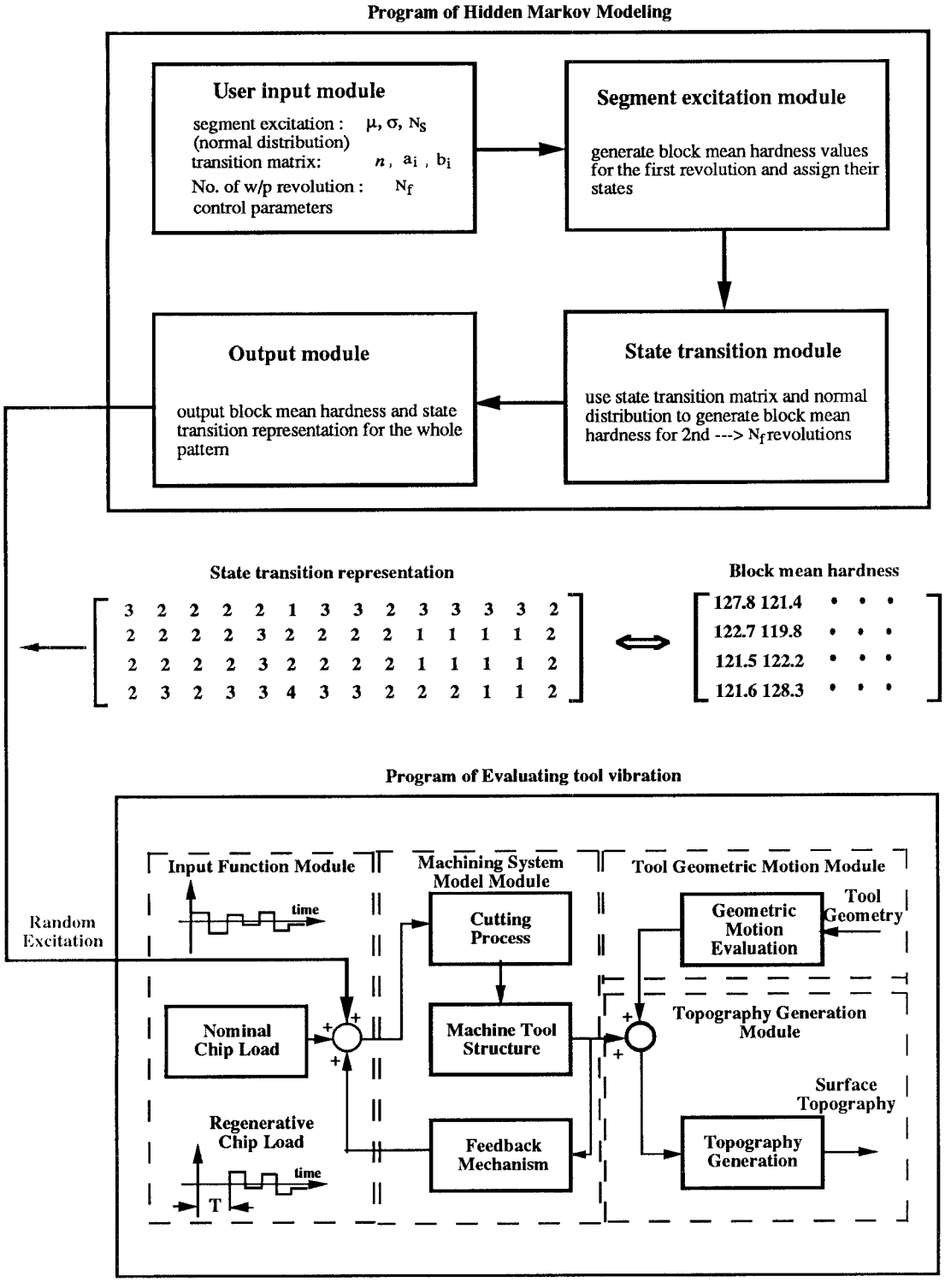

Fig. 6. Methodology to Simulate the Topography of a Machined Surface

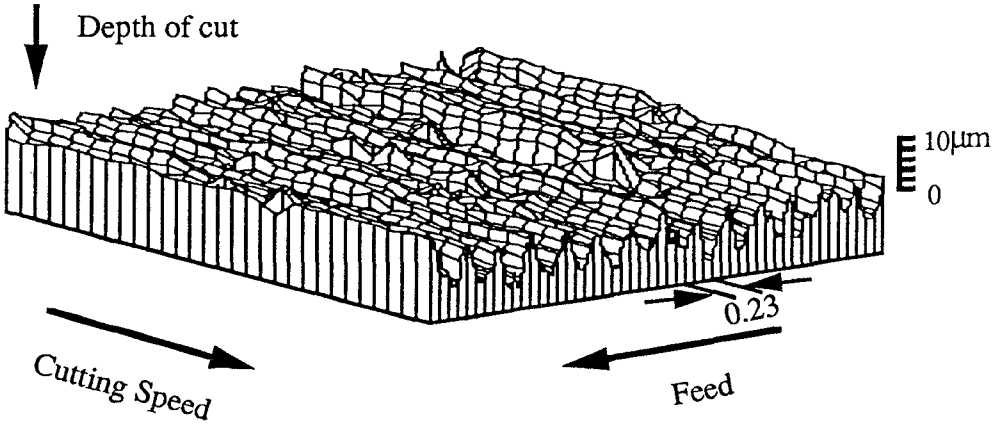

(a) Measured

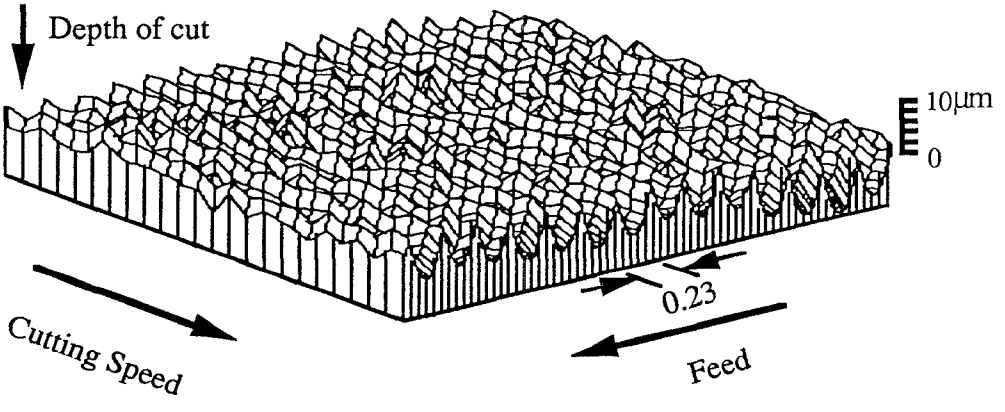

(b) Simulated (segment exitation only)

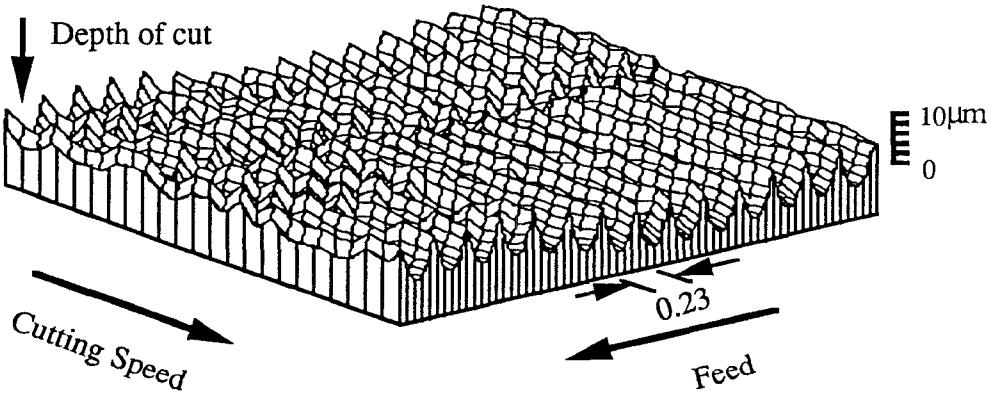

(c) Simulated (hidden Markov modeling)

Fig. 7. Surface Topography Comparison

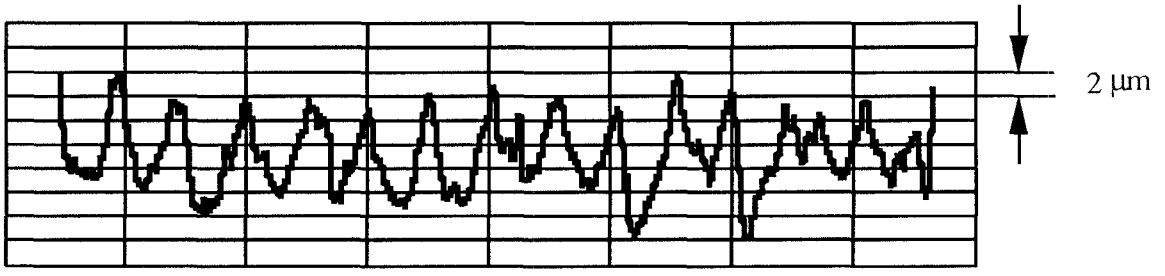

(a) Measured (Ra = 4.11 μm)

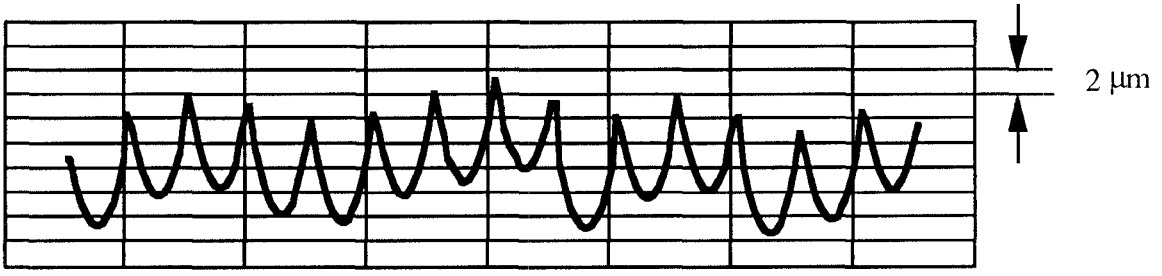

(b) Segment Excitation Model (Ra = 4.07 μm)

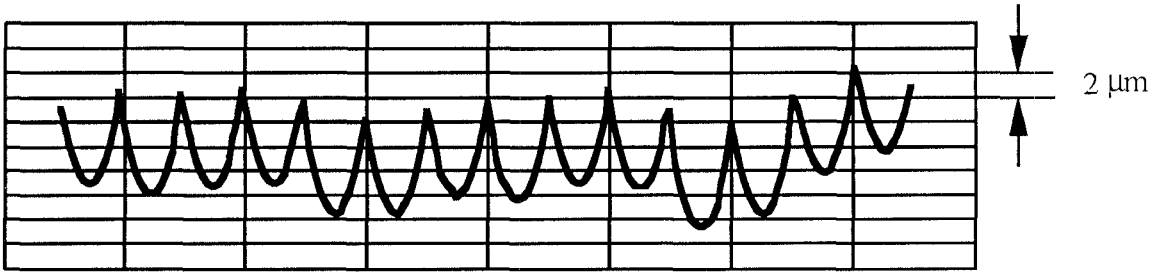

(c) Hidden Markov Model (Ra = 4.09μm)

Fig. 8. Surface Profile Comparison

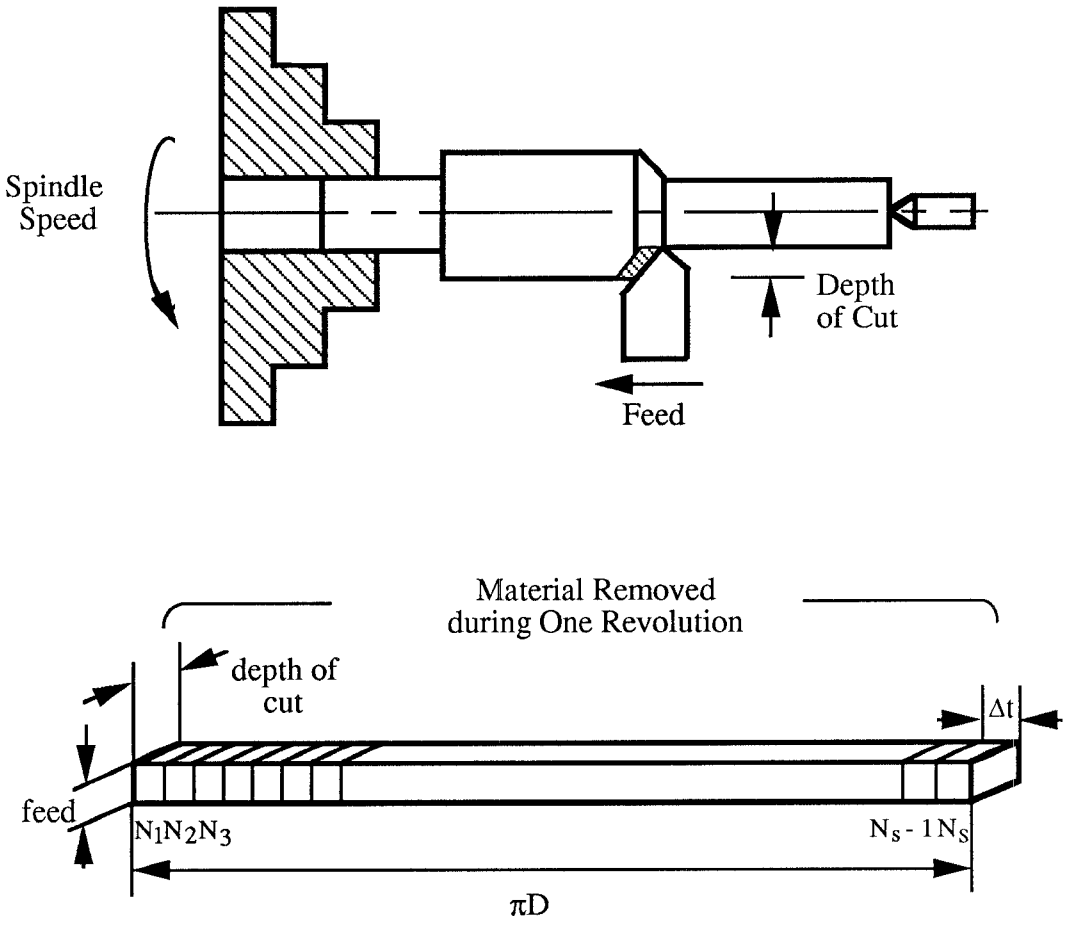

Fig. 1 Mechanism of Random Excitation

Table 1. Ra Values of the Measured and Simulated Surface Topographies

	Measured	Segment Excitation	Hidden Markov Model (0.3,0.4,0.3)		Hidden Markov Model (0.2,0.6,0.2)	
	(μm)	(μm)	state=4 (μm)	state=10	state=4 (μm)	state=10
	4.54	4.19	4.17	3.69	3.75	3.65
	4.38	3.73	4.42	3.72	3.89	3.66
	4.60	3.72	4.22	3.67	3.92	3.66
	4.54	4.00	4.43	3.75	3.72	3.65
	4.21	3.78	4.19	3.66	3.76	3.70
	4.03	3.97	4.14	3.72	3.86	3.68
	4.10	3.73	4.62	3.67	3.84	3.70
	3.65	3.79	3.97	3.71	3.86	3.67
	4.25	4.07	3.95	3.69	3.70	3.66
	4.40	4.03	4.09	3.73	4.00	3.66
	3.80	3.78	4.49	3.68	3.82	3.69
	3.74	3.92	4.19	3.69	3.73	3.67
	4.28	3.80	4.05	3.69	3.70	3.66
	4.51	4.04	4.34	3.71	3.89	3.69
	4.73	3.88	4.10	3.70	3.76	3.68
	4.64	3.82	4.47	3.69	3.85	3.69
	4.08	3.89	4.09	3.70	3.87	3.65
	4.10	3.98	4.15	3.65	3.77	3.69
	3.91	4.00	4.15	3.73	4.48	3.66
	4.54	3.81	4.08	3.71	4.37	3.66
	4.52	3.93	4.50	3.71	3.87	3.69
	3.64	4.11	4.10	3.70	3.81	3.64
	4.01	4.11	4.41	3.70	3.84	3.69
	4.06	3.84	4.42	3.69	3.86	3.70
	4.18	3.95	4.31	3.68	3.89	3.70
Mean	4.22	3.92	4.24	3.70	3.87	3.67
Std.	0.32	0.13	0.17	0.02	0.18	0.02